The Swiss Alps and their peripheral foreland basin: Stratigraphic response to deep crustal processes

O. A. Pfiffner

Institute of Geological Sciences, University of Bern, Bern, Switzerland

F. Schlunegger

Geologisches Institut, ETH-Zentrum, Zürich, Switzerland

S. J. H. Buiter

Institute of Geological Sciences, University of Bern, Bern, Switzerland

Received 30 May 2000; revised 11 January 2002; accepted 18 January 2002; published 30 April 2002.

[1] This paper gives a synoptic view of the Cenozoic evolution of the Swiss Alps and their northern foreland basin. In this orogen, deep crustal processes (subduction, nappe stacking, underplating, and exhumation) are intimately linked with surface processes (surface uplift, erosion, basin formation, and basin-axis migration). Within the foreland basin the spatial pattern of subsidence and alluvial fan construction suggests that an increase in flexure of the foreland plate and the creation of relief in the orogen migrated from east to west in the course of collision. In the orogen itself, crustal thickening involved lower crust of the Adriatic margin in the east and the European margin in the west. Exhumation of upper crustal units occurred earlier in the east as compared with the west. An Adriatic mantle wedge (the Ivrea body) and its associated wedge of lower crustal material are identified as an extra lithospheric load which contributed to downward flexure of the European plate. As a result of enhanced subsidence of the foreland plate, relief was generated presumably in order to adjust to critical taper geometry. It appears, therefore, that the westward motion of the Adriatic wedge ultimately caused the contemporaneous westward propagation of the location of enhanced rates of alluvial fan construction. Coeval strike-slip and N-S convergence juxtaposed the Adriatic wedge sequentially to different European upper crustal units which resulted in different styles of crustal structure and evolution along strike within the orogen. *INDEX TERMS:* 8102 Tectonophysics: Continental contractional orogenic belts; 8150 Tectonophysics: Plate boundary—general (3040); 9335 Information Related to Geographic Region: Europe; *KEYWORDS:* Swiss Alps, foreland basin, flexure, subsidence, Ivrea, crustal structure

1. Introduction

[2] The geometry of lithospheric downwarping during collision between two plates results from a complex interaction between surface loads which are added as the orogen grows (topographic loads), deep lithospheric loads acting on the downgoing lithosphere, and slab pull [*Turcotte and Schubert*, 1982]. Topographic loads form in geodynamic settings where the material flux down the subduction zone is less than the incoming flux. This results in the buildup of an orogenic wedge with a pro-wedge on the incoming side, and a retro-wedge on the opposite side [*Beaumont et al.*, 1999]. These wedges grow by incorporation of accreted material scraped off the incoming plate. Material entering the wedge gets deformed, uplifted, and exhumed. Deep lithospheric loads are the result of the replacement of light continental upper crust by denser rocks of lower crustal or mantle origin as continent-continent collision proceeds.

[3] *Karner and Watts* [1983], *Lyon-Caen and Molnar* [1989], and *Royden* [1993] explored the forces that cause the present deflection of the North Alpine foreland (Molasse Basin) of the Swiss Alps. Using flexural models, *Royden* [1993] concluded that the present-day shape of the Swiss Alps (i.e., the topography and the large-scale structures at depth) can be explained by a combination of topographic loads (i.e., Alpine edifice made up of a nappe stack of upper crustal material) and deep lithospheric loads (i.e., mantle loads at depth). Royden, however, did not consider the situation between the Oligocene and the Miocene.

[4] The flexural pattern of the foreland on the opposite side (South Alpine foredeep, Po Basin) was recently explored by *Bertotti et al.* [1998]. They found that the curvature of the loaded plate increased between the late Paleogene and the Tortonian, suggesting progressive weakening of the flexed plate. *Bertotti et al.* [1998] thought that the inferred weakening was caused by a practically complete decoupling of the upper-middle crust from its mantle substratum as orogenesis proceeded.

[5] Between the Oligocene and the Miocene the evolution of the Alps changed from a phase of frontal accretion to a phase of internal thickening. An understanding of the driving forces for that time will therefore significantly enhance our knowledge about the Alpine system (which includes the foreland basins).

[6] In this paper we relate the three-dimensional deflection geometry of the North European foreland plate of the Swiss Alps between the early Oligocene and the middle Miocene to deep crustal processes. Specifically, we discuss the role that a dense lower crustal and mantle wedge, which was forced into the light upper European crust, played in basin formation processes. The location of the wedge and the subduction geometry was reconstructed for the late Oligocene and the early and middle Miocene, using data about the chronology and the magnitude of crustal shortening in the Swiss Alps [*Schmid et al.*, 1996, 1997]. These

0278-7407/02/2000TC900039

time slices were selected on the basis of well-defined stratigraphic sections [e.g., *Kempf et al.*, 1998] and crosscutting relationships between temporally calibrated metamorphic fabrics and tectonic structures of the evolving Alps [*Schmid et al.*, 1997]. Reconstruction of the deflection geometry of the foreland plate was done using a compilation of published compacted thicknesses of foreland sequences. Additionally, we synthesized the temporal and spatial evolution of the large-scale drainage pattern of the foreland, which bears information about the formation of relief of the rising Alps and the regional tilt of the foreland basin.

2. Geologic Setting

[7] The Swiss Alps, also referred to as the central Alps, form the transition between the E-W striking Eastern Alps and the N-S striking Western Alps. The North Alpine foreland basin straddles the Eastern Alps in the north and merges with the Vienna Basin in the east. It narrows going west, such that it pinches out in the Western Alps. In the segment of the Swiss Alps it forms the classical Molasse Basin (Figure 1). The Jura Mountains, an external fold and thrust belt of the Alps, formed in the most distal part of the Molasse Basin. Shortening associated with the Jura Mountains is linked at depth to the Alps, making the Molasse Basin, in fact, a piggyback basin. To the south of the Swiss Alps, we find the Po Basin, a peripheral foredeep shared by the Apennines and the Alps (Figure 1).

2.1. The Alps

[8] The Swiss Alps contain a number of nappe systems that have traditionally been grouped according to the paleogeographic parentage of their Mesozoic sedimentary sequences. The Helvetic nappes (Figure 1) represent the former shelf and slope areas of the European margin. The Penninic nappes contain remnants of three domains: (1) the Valais trough, a basin that formed in the distal stretched part of the European margin, (2) the swell region of the Briançonnais microcontinent, and (3) the Piemont ocean, a narrow transform-fault dominated ocean that opened between the Eurasian and Adriatic-African plates in Jurassic times. The Austroalpine nappes together with the Southalpine nappes (often referred to as Southern Alps) represent the subsided margin of the Adriatic (or Apulian) microplate, which is here considered as a promontory of the African plate [*Channell*, 1992].

[9] The shallow crustal structure of the Swiss Alps has been studied extensively by numerous geologists in the past. Structural work revealed a bivergent nappe stack (Figures 2a and 2b). In the Helvetic and Penninic nappes, thrusting was north directed. The nappe stack contains three types of nappes: (1) thrust sheets made up of crystalline basement, (2) thrust sheets consisting of Mesozoic-Cenozoic sediments, and (3) thrust sheets containing Mesozoic ophiolites and associated oceanic sediments [*Pfiffner*, 1993b; *Schmid et al.*, 1996]. In the Southern Alps, thrusting was south directed, and the nappe stack involves two types of thrust sheets: crystalline basement and Mesozoic-Cenozoic sediments [*Schumacher et al.*, 1997]. The Austroalpine nappes overly the Penninic nappes. Their evolution is due to a more complex deformation pattern characterized by compression and extensional collapse [*Froitzheim et al.*, 1997]. At a deeper level the Alps display an asymmetric structure with lower crust and lithospheric mantle of the European margin being subducted beneath equivalent units of the Adriatic margin [*Pfiffner et al.*, 1997a].

2.2. North Alpine Foreland Basin

[10] The stratigraphic development of the peripheral North Alpine foreland basin (Figure 1) can be described in terms of early turbiditic deep-water sediments (underfilled Flysch stage, Late Cretaceous to Eocene) and later shallow-water/continental sediments (overfilled Molasse stage, Oligocene to Miocene) [*Sinclair and Allen*, 1992; *Lihou and Allen*, 1996]. These sediments accumulated on a Mesozoic sequence of marls and carbonates that form the sedimentary cover of the North European foreland plate [*Sinclair et al.*, 1991]. The Molasse deposits, which represent the late overfilled stage of the evolution of the North Alpine Foreland Basin [*Sinclair and Allen*, 1992; *Sinclair*, 1997a], have traditionally been divided into four lithostratigraphic groups that form two shallowing and coarsening upward stratigraphic sequences [*Matter et al.*, 1980]. The oldest sequence comprises the early Oligocene (34–30 Ma) Lower Marine Molasse group (Untere Meeresmolasse (UMM)), which is overlain by the late Oligocene to early Miocene (~30–20 Ma) fluvial clastics of the Lower Freshwater Molasse group (Untere Süsswassermolasse (USM)). During these times, drainage systems with sources in the evolving Alps were transverse within the Alps, but turned orogen-parallel into a northeastward flowing axial submarine (UMM) or terrestrial (USM) drainage [*Füchtbauer*, 1964; *Sinclair*, 1997b]. The second sequence started with deposition of the 20–16.5-Myr-old shallow-marine sandstones of the Upper Marine Molasse group (Obere Meeresmolasse (OMM)). These deposits interfinger with large fan-delta deposits adjacent to the thrust front [*Homewood et al.*, 1986; *Keller*, 1989; *Kempf et al.*, 1998]. The second sequence ended with accumulation of fluvial clastics of the Upper Freshwater Molasse group (Obere Süsswassermolasse (OSM)) at ~13.5 Ma. During deposition of the OSM, the orogen-normal Alpine paleorivers drained into a southwestward flowing orogen-parallel (OSM) drainage [*Matter et al.*, 1980].

[11] Along the southern border of the foreland basin, the Molasse deposits are present in a stack of southward dipping thrust sheets referred to as Subalpine Molasse in classic Alpine literature (Figure 1). The Plateau Molasse, which represents the more distal part of the basin, is mainly flat lying and dips gently toward the Alpine orogen. Thrusting in the Subalpine Molasse was contemporaneous with sedimentation [*Homewood et al.*, 1986; *Pfiffner*, 1986; *Kempf et al.*, 1998].

3. Structure and Evolution of the Alpine Orogen

3.1. Crustal Structure in Profile View

[12] The crustal structure of the Swiss Alps is known in some detail owing to a wealth of geophysical data, involving refraction and reflection seismic data, as well as extensive structural work. The most recent data, which were in part gathered in the framework of the National Research Program NRP 20, are compiled by *Pfiffner et al.* [1997a].

[13] The crustal structure is displayed in Figure 2 along three transects. Two transects (Figures 2a and 2b) are orogen normal and show a nappe stack of upper crustal units overlying an asymmetric subduction zone that involves lower crust and mantle lithosphere. The third transect (Figure 2c) is orogen parallel and shows the lateral variation of the crustal structure.

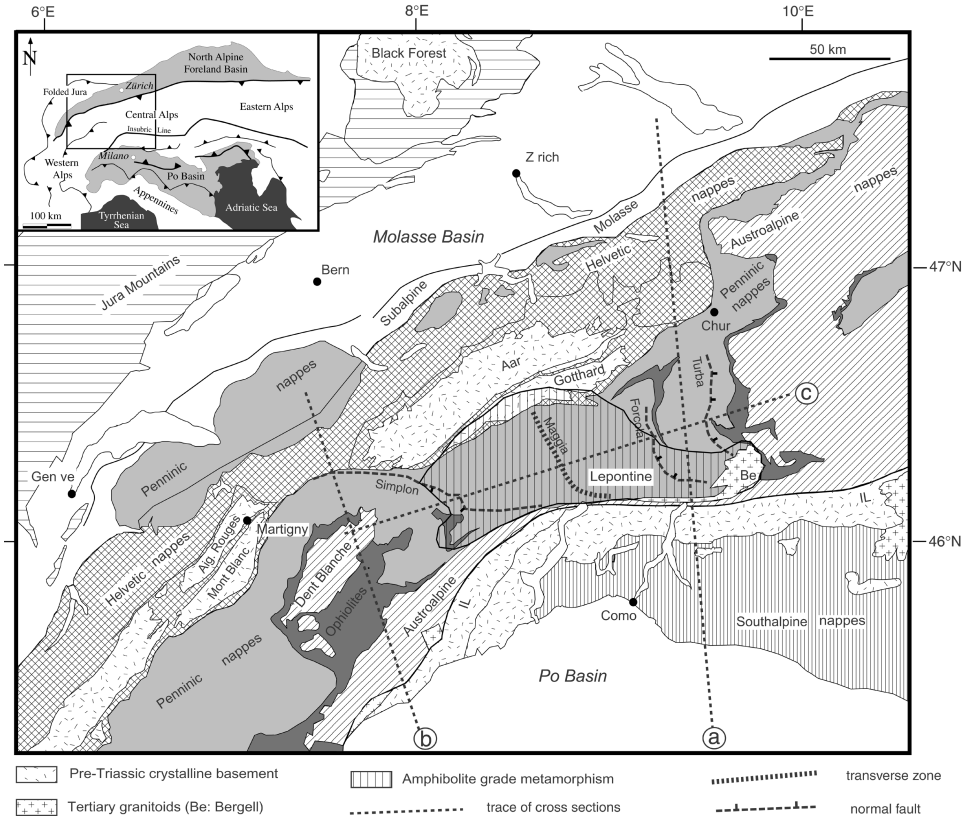

Figure 1. Tectonic sketch map of the Alpine orogen and its foreland basins. The complex patterns of the various Alpine units are due to variations in axial plunge and interference with topography effects. Inset shows the Swiss Alps within the larger framework of the Alps. Thin dotted lines indicate traces of the cross sections of Figure 2 (see circled letters a, b, and c).

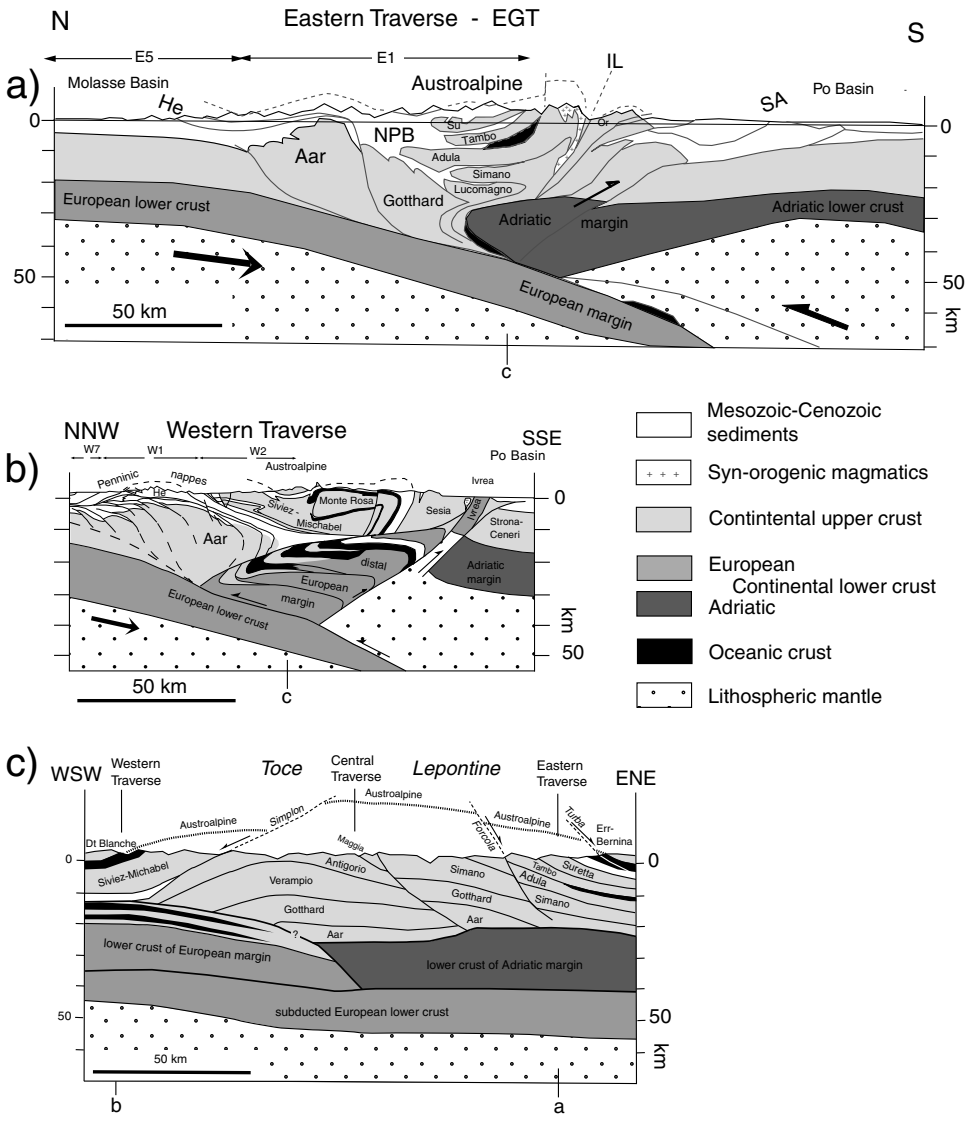

Figure 2. Cross sections through the Swiss Alps showing crustal structure (traces are given in Figure 1). (a) Geologic profile following the European GeoTraverse EGT and the Eastern Traverse of NRP 20. It shows a bivergent nappe stack overlying an asymmetric subduction zone and a wedge of Adriatic mantle and lower crust (modified from *Pfiffner et al.* [2000]). E1 and E5, seismic lines; He, Helvetic nappes; Su, Suretta nappe; NPB, North Penninic Bündnerschiefer; IL, Insubric Line; Or, Orobie thrust sheet; SA, Southalpine nappes. (b) Geologic profile following the Western Traverse of NRP 20, extended southward into the Po Basin. South directed thrusting in the upper crust is much less pronounced in comparison with Figure 2a. The subducted lower European crust is overlain by a wedge consisting of Adriatic mantle and European lower crust. Seismic lines are labeled W1, W2, W7. (c) Geologic profile along strike the Swiss Alps. The nappe stacks vary along strike and are cut by normal faults (Simplon to the west, and Forcola and Turba to the east). The exact location of the transition from the European to the Adriatic wedge overlying the subducted European crust is speculative.

[14] Figure 2a follows the Eastern Traverse of NRP 20 and the European GeoTraverse (EGT) [*Pfiffner and Hitz*, 1997; *Schmid et al.*, 1997]. The cross section shows that the European lithospheric mantle and the lower crust of the European margin have been subducted beneath the Adriatic lithosphere. Doubling of the Moho is observed in seismic data to a depth of around 70 km. The Adriatic lower crust forms a wedge whose tip is overlain and underlain by crust of European provenance. The thickness of this lower crustal wedge is larger than the thickness of the lower Adriatic crust observed farther south, which suggests that deformation shortened and thickened it. An Adriatic mantle wedge overlies the lower crust of the subducted European margin. The upper crust is thickened by imbricate thrusting, which is north vergent north of the Insubric Line and south vergent to the south of it. The Insubric Line itself is a major fault with a reverse and strike-slip component [*Schmid and Kissling*, 2000]. The basal thrusts of the units to the north of the Adriatic lower crustal wedge and the Insubric Line are overprinted by ductile folding (postnappe folding in Alpine literature). Synorogenic magmatics of Cenozoic age (Bergell intrusion) intruded just north of the Insubric Line. The European crust was decoupled from its lower crustal substratum and subsequently shortened and thickened by imbricate thrusting. The northernmost unit, the Aar massif, forms a broad antiform with a steeply south dipping southern limb. Two foredeeps filled by Cenozoic clastics can be recognized: the Molasse Basin in the north, and the Po Basin in the south. Both foredeeps are synorogenic in nature as indicated by Helvetic and Southalpine thrust sheets that now overly their proximal parts.

[15] Figure 2b is a cross section following the Western Traverse of NRP 20 [*Escher et al.*, 1997; *Pfiffner et al.*, 1997b], but has been extended south into the Po Basin for this paper. Similar to the situation in the east (Figure 2a), the lower crust of the European margin extends to beneath the Adriatic mantle wedge. Lower crust of the distal European margin and the originally adjacent Valais and Briançonnais units is, however, piled up in front of this mantle wedge. The general distribution of mantle and lower crustal rocks is in accordance with geophysical data [*Valasek*, 1992; *Valasek and Mueller*, 1997], but we interpret the provenance of the lower crustal wedge differently. Unlike farther east, the Adriatic upper crust in this section shows much less shortening at the surface and therefore requires a much smaller volume of lower crust to obtain a balanced section. Thus we conclude that the lower crustal wedge, as defined by geophysical data, is derived from the European crust and not from the Adriatic as proposed by *Escher et al.* [1997]. Our interpretation resembles the situation in the French-Italian Western Alps as discussed by *Schmid and Kissling* [2000]. The Ivrea lower crustal section corresponds to the deformed front of the Adriatic wedge. The upper crustal section north of the Ivrea zone is characterized by imbricate thrusting and by the occurrence of large-scale back-folds which affect the Monte Rosa and adjacent units, as well as the southern part of the Aar massif basement uplift.

[16] The internal structure of the Penninic nappes of the two transects differs in style. Both styles can be traced toward the Maggia transverse zone, which is located between the two transects (Figure 1). A correlation of individual tectonic units across the Maggia transverse zone, however, is not possible (Figure 2c). The Maggia "nappe" itself has a synformal structure striking NNW-SSE, i.e., perpendicular to the regional strike [*Merle et al.*, 1989; *Klaper*, 1990; *Pfiffner et al.*, 1990].

[17] The cross section in Figure 2c shows the variation in crustal structure in profile view along strike of the Alpine orogen. The Maggia transverse zone is located between the high-grade Lepontine and Toce areas. Exhumation of these terranes was associated with normal faulting along east and west dipping normal faults (Turba, Forcola, and Simplon faults) [cf. *Mancktelow*, 1992; *Nievergelt et al.*, 1996; *Meyre et al.*, 1998]. Within the upper crust, the Aar and Gotthard basement blocks can be traced along strike with some certainty, whereas the Simano-Adula (Figure 2a), and the Verampio-Antigorio nappes (Figure 2c) cannot be taken as direct equivalents and differ in style considerably. These basement blocks, although pertaining to the same Penninic nappe system, evolved independently, with the Maggia transverse zone acting as a lateral ramp structure. As will be discussed in section 3.3, nappe stacking and exhumation of the Penninic units occurred at an earlier time in the Lepontine area and the Eastern Traverse compared with the Toce area and the Western traverse.

[18] At the level of the lower crust, the cross section of Figure 2c shows the juxtaposition of two blocks consisting of European and Adriatic lower crust, which overlie the subducted European lower crust. The boundary geometry between the two wedges as shown in Figure 2c is speculative, but it intends to show a wrench fault zone separating two independently moving blocks.

3.2. Three-Dimensional Crustal Structure

[19] Extensive coverage of the Swiss Alps by the seismic lines of NRP 20 and earlier studies allowed the development of a three-dimensional (3-D) model of the crustal structure [see, e.g., *Valasek and Mueller*, 1997; *Waldhauser et al.*, 1998; *Schmid and Kissling*, 2000]. The 3-D geometry of this crustal structure is shown in Figure 3 by means of structure contour maps of the interface between upper and lower crust (Conrad discontinuity) and the crust-mantle boundary (Moho).

[20] Figure 3a shows the 3-D geometry of the Conrad discontinuity. The Conrad velocity discontinuity is taken as the top of the lower crust (with velocities of 6.5 km/s) underlying upper crust with velocities of 5.9–6.2 km/s [*Valasek and Mueller*, 1997]. Along the sector of the Eastern and European GeoTraverse (trace "a") the European Conrad discontinuity dips gently south to beneath the tip of the Adriatic lower crustal wedge. Within the Adriatic crust the Conrad discontinuity forms an elongate high approximately beneath the trace of the Insubric Line. Along the Western Traverse (trace "b") the overall structure remains similar, but the structure contours turn into a N–S trend south of the Mt. Blanc basement uplift and follow the general strike of the Western Alps of France and Italy. As discussed in section 3.1, the lower crustal wedge between the Ivrea zone and the Aar and Mt. Blanc basement uplifts consists of European derived lower crust. Therefore, when going along strike to the east, there must be a boundary where European lower crust is replaced by Adriatic lower crust. In Figure 3a this limit is put just north of the eastern end of the Ivrea zone and corresponds to the position where shortening within the Adriatic crust, and thus the necessity for a lower crustal wedge for reasons of geometric balancing, is tapering off going west.

[21] Figure 3b illustrates the shape of the crust-mantle boundary. The European Moho dips gently SSE. The Adriatic Moho on the other hand forms an E–W striking elongate high 100 km south of the Insubric Line, with a depression in the area where the EGT

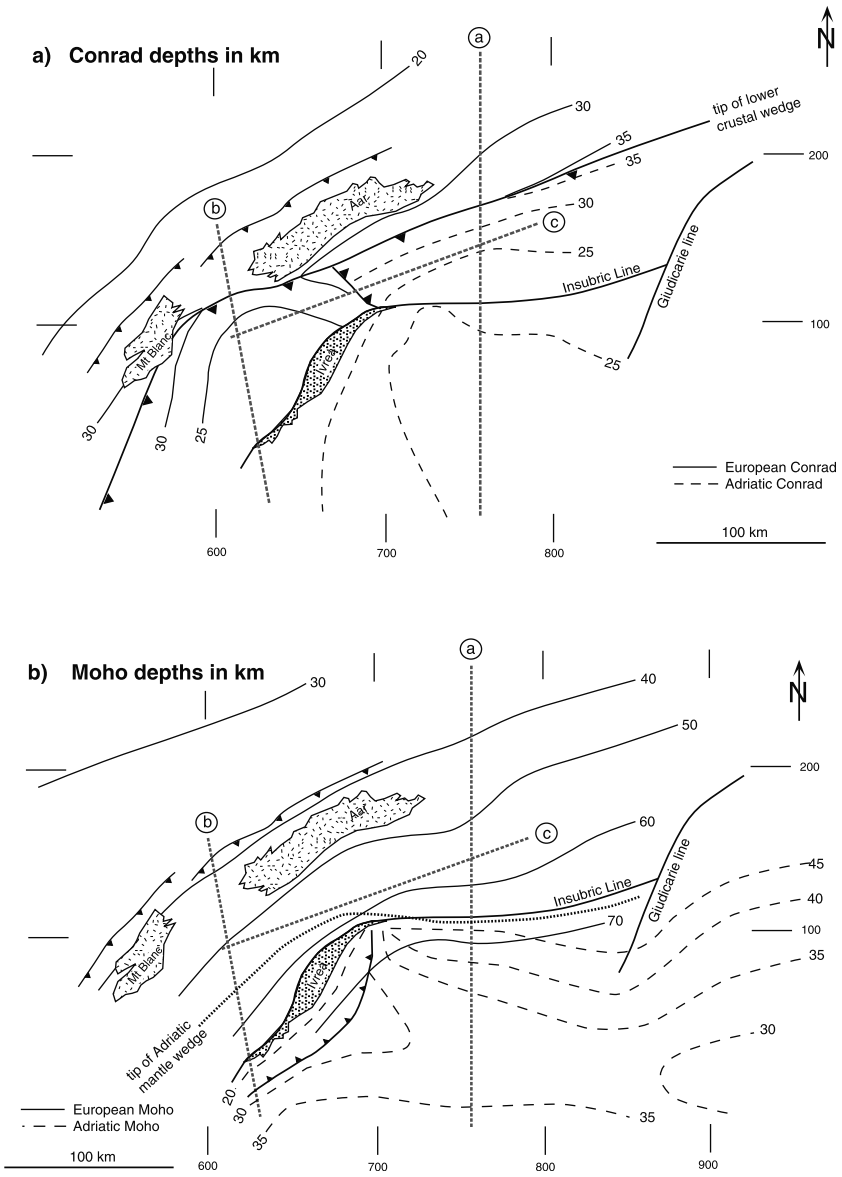

Figure 3. Three-dimensional crustal structure of the Swiss Alps displayed as structure contour maps (based on *Waldhauser et al.* [1998] and *Schmid and Kissling* [2000]). Grid numbers refer to the Swiss national kilometer grid. Thin dotted lines indicate traces of the cross sections of Figure 2 (see circled letters a, b, and c). (a) The Conrad discontinuity (between lower and upper crust) displays a complex geometry with varying dips and strike, particularly for the European crust. (b) The Moho (crust/mantle boundary) displays a particularly complex shape within the Adriatic plate.

crosses. The elongate high extends westward toward the outcropping Ivrea zone. Here the Moho is doubled and raised by thrust faulting and almost reaches the Earth's surface. The tip of the Adriatic mantle wedge straddles the Insubric Line, but then extends beyond the Ivrea Zone into the Western Alps.

3.3. Evolution

[22] The Swiss Alps are the result of two orogenies, a Cretaceous orogeny with mainly ENE–WSW convergence, and a Cenozoic orogeny which resulted from N–S convergence. A summary of the timing of the deformation phases is given by *Schmid et al.* [1996, 1997] for the eastern Swiss Alps, by *Escher et al.* [1997] for the western Swiss Alps, and by *Schumacher et al.* [1997] for the Southern Alps. The Cretaceous orogeny involved an eastward dipping subduction zone, which ultimately led to the building of the Western Alps of France and Italy and the Eastern Alps of Austria. In the central Alps of Switzerland, sedimentation continued up into the Eocene, which implies that the Helvetic and Southalpine as well as part of the Penninic nappes were not affected by this orogeny [see, e.g., *Pfiffner*, 1992].

[23] A compilation of the orogenic events in the Swiss Alps between the Eocene and the present is summarized in Figure 4. Along the transect through the eastern Swiss Alps (Figure 4a) one recognizes that synorogenic sedimentation, preserved as Flysch and Molasse deposits, migrated from the orogen axis outward in

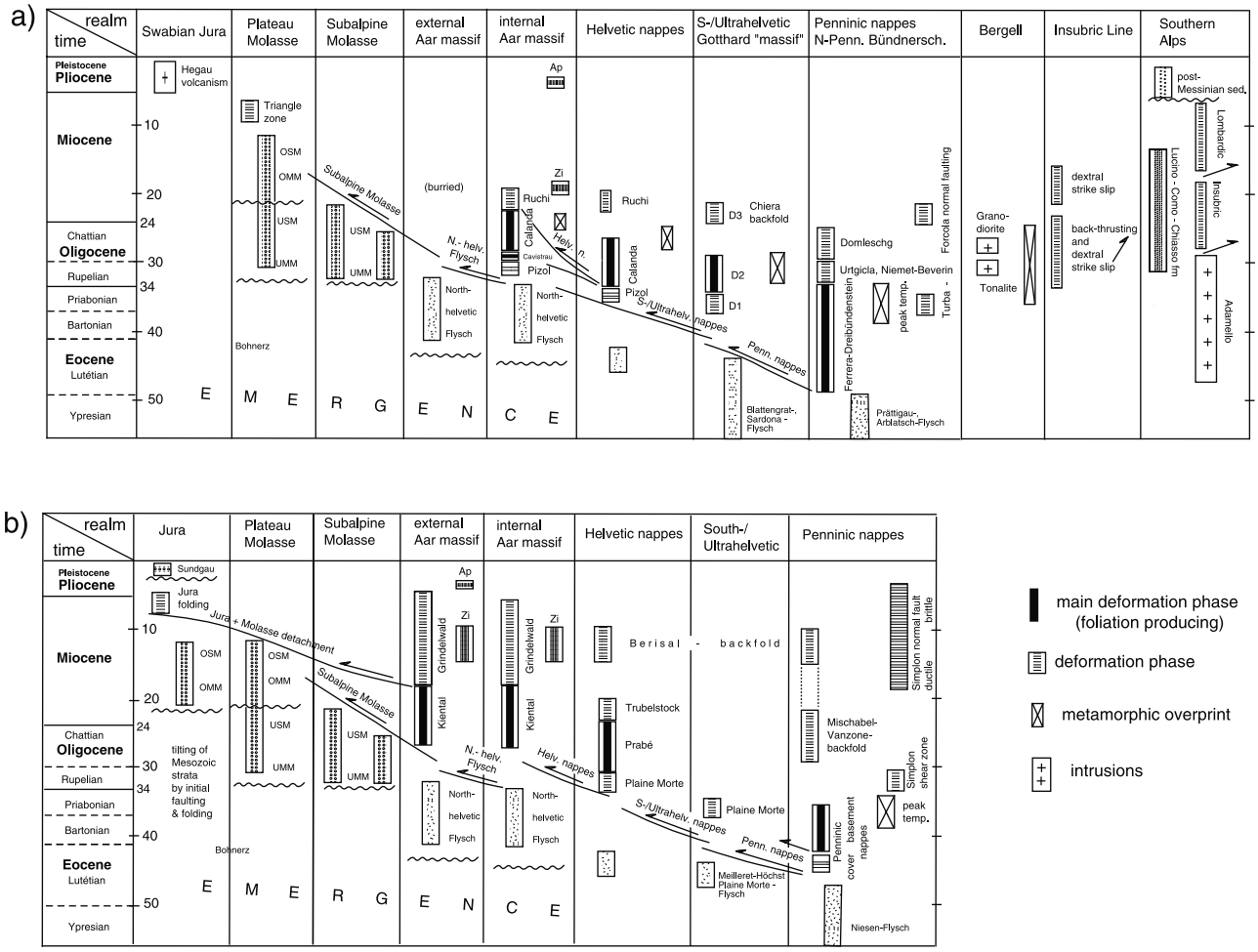

Figure 4. Timetable summarizing the main orogenic events (sedimentation, deformation phases, magmatism, metamorphism). Abbreviations are as follows: UMM, Lower Marine Molasse; USM, Lower Freshwater Molasse; OMM, Upper Marine Molasse; OSM, Upper Freshwater Molasse; Ap, apatite cooling age; Zi, zircon cooling age. (a) Eastern Swiss Alps (modified from *Schmid et al.* [1997]). Local deformation phases are labeled D1, D2, D3. (b) Western Swiss Alps (in part after *Escher et al.* [1997]). In general, deformation migrated from internal to external zones, whereby the latest phases affected the Molasse and Po Basins.

time. Sedimentation in these foredeeps evolved from earlier, Cretaceous Flysch basins and persisted longer, up into Pliocene times in the Southern Alps. The main deformation phase is oldest in the center of the orogen (Eocene Ferrera phase in the Penninic nappes) and migrated outward to the north reaching the Helvetic nappes and the Aar massif in Oligocene and the Molasse Basin in Miocene times. During the same time, deformation migrated also to the south, involving Oligocene back thrusting along the Insubric Line and the Oligocene and Miocene Insubric and Lombardic phases in the Southern Alps. The phase of back thrusting was coeval with extensional faulting along the east dipping Turba and Forcola normal faults prior to 30 Ma and at circa 24 Ma, respectively. Peak temperatures were reached after this nappe stacking phase. A late phase of backfolding affected the area south of the Gotthard thrust sheet (Chiera backfold), where thrust faults and foliations were passively rotated into a steep to overturned position.

[24] In the western Swiss Alps a scheme similar to the one in the east is recognizable (see Figure 4b). Folding of the Jura Mountains is the youngest event in the north. It was probably responsible for a clockwise rotation of 7°–14° after 14 Ma [*Kempf et al.*, 1998] of the entire Molasse Basin during piggyback transport. Two phases of backfolding, Mischabel-Vanzone (in the Penninic nappes), followed by Berisal (affecting the southern Gotthard thrust sheet and adjacent units), can be distinguished (see also Figure 2b). Berisal backfolding occurred contemporaneously with extensional activity along the west dipping Simplon normal fault.

[25] A comparison of the events in the east and west reveals similar ages for the Flysch and Molasse stages of the foreland basin evolution. Also, the general sequence of the main deformation phases for the Penninic and Helvetic nappes is similar, although in absolute ages the western Swiss Alps seem to have evolved some 5 Ma after their eastern equivalent. Complementary to this diachronous thrusting and nappe stacking, a remarkable set of coeval deformation events of highly variable style can be recognized. For example, back thrusting along the Insubric Line was contemporaneous to backfolding of the Gotthard basement block, thrusting in the Helvetic zone and the onset of thrusting in the Subalpine Molasse. It was also coeval with Mischabel-Vanzone backfolding

Table 1. Stratigraphic Data of the Molasse Basin[a]

Well/Section	Compacted Thicknesses, m			
	30–25 Ma	25–20 Ma	20–16.5 Ma	16.5–13.5 Ma
TS, Tschugg-1	250	>250	–	–
R, Ruppoldsried-1	400	>500	–	–
L, Linden-1	1600	1600	1000	–
T, Thun-1	2150	1950	–	–
A, Althishofen-1	120	800	>300	–
E, Entlebuch-1	500	2100	–	–
EM, Emme	1200	–	–	–
HO, Honegg	1500	–	–	–
S, Schafisheim	0	>250	–	–
BO, Boswil-1	350	720	460	–
HÜ, Hünenberg-1	450	1140	990	–
R, Rigi	3600	–	–	–
EI, Einsiedeln	2700	–	–	–
N, Necker	1950	2050	–	–
S, Steintal	1700	–	–	–
B, Berlingen-1	0	700	200	–
K, Kreuzlingen-1	0	1000	200	–
LI, Lindau-1	0	1050	300	–
KÜ, Künsnacht-1	0	1500	550	–
BF, Brochene Fluh	0	>100	–	–
HÖ, Höhronen	–	2000	–	–
N, Napf	–	–	1050	850
H, Hörnli	–	–	1000	650
Z, Zürich	–	–	–	600

[a]A compilation and discussion of the data in terms of temporal resolution are presented by *Schlunegger* [1999]. Additional data are taken from *Kempf et al.* [1999] for the Hörnli, Necker, and Steintal sections, and from *Kempf and Matter* [1999] for the Zurich section.

in the west. In late Miocene times the youngest thrusting phase in the east (Lombardic phase in the Southern Alps) was coeval with (1) the formation of the triangle zone between the Subalpine Molasse and the Plateau Molasse in the east, (2) the formation of the Jura Mountains, (3) uplift of the Aar massif (Grindelwald phase), and (4) the brittle activity along the Simplon normal fault in the west.

4. Architecture of the North Alpine Foreland Basin

4.1. Assessing the Basin Architecture

[26] In order to assess the deflection of the North Alpine foreland plate we constructed isopachs maps for the time intervals between 30–25 Ma, 25–20 Ma (USM), 20–16.5 Ma (OMM), and 16.5–13.5 Ma (OSM). The isopach maps are based on the thicknesses of sections that were measured at outcrop and in wells (Table 1). The sections which are located in the folded and thrusted part of the Molasse were restored to their palinspastic position using the available information about the timing and amount of shortening [*Schlunegger et al.*, 1993, 1997; *Kempf et al.*, 1998]. Mapping of the isopachs was achieved by assuming constant thickness gradients between locations where stratigraphic data is available.

[27] The spatial pattern of initiation of alluvial fan construction is an important proxy for orogen-parallel variations in crustal processes in the Alps. We therefore synthesized data regarding the spatial pattern of initiation of conglomerate deposition. These data are taken from stratigraphic studies of *Kempf et al.* [1999] for eastern Switzerland, *Schlunegger et al.* [1996] for central, and *Berger* [1996] for western Switzerland. Paleoflow directions which bear information about the regional tilt of the basin were taken from *Diem* [1986] for the UMM and from *Matter et al.* [1980], *Schlunegger et al.* [1993], and *Kempf et al.* [1999] for the succeeding units. The distal border of the Molasse deposits at 30 Ma and in succeeding time steps is taken from palinspastic restorations [*Homewood et al.*, 1986; *Schlunegger et al.*, 1993, 1997; *Kempf et al.*, 1998].

4.2. Three-Dimensional Evolution of Basin Architecture

[28] The spatial pattern of the onset of alluvial fan construction, i.e., the first occurrence of thick-bedded conglomerates within the Swiss part of the North Alpine foreland basin, is presented in Figure 5, together with the distal pinch-out and paleoflow directions during UMM times. It shows a westward shift of the location of the first occurrence of thick-bedded conglomerates as alluvial fan construction started prior to 31 Ma in the east, at ~30 Ma in the central part of the basin, and some 4 Myr later in the west. Figure 5 also implies an eastward tilt of the foreland plate prior to 30 Ma indicated by the NE-SW orientation of the distal pinch-out of the UMM. The east directed tilt of the foreland plate is also reflected by the east directed paleoflow drainage.

[29] We use the structure contours of the base of the foreland strata as proxy for the deflection of the foreland plate through time. Figure 6 shows the situation at 25, 20, 16.5, and 13.5 Ma. It also

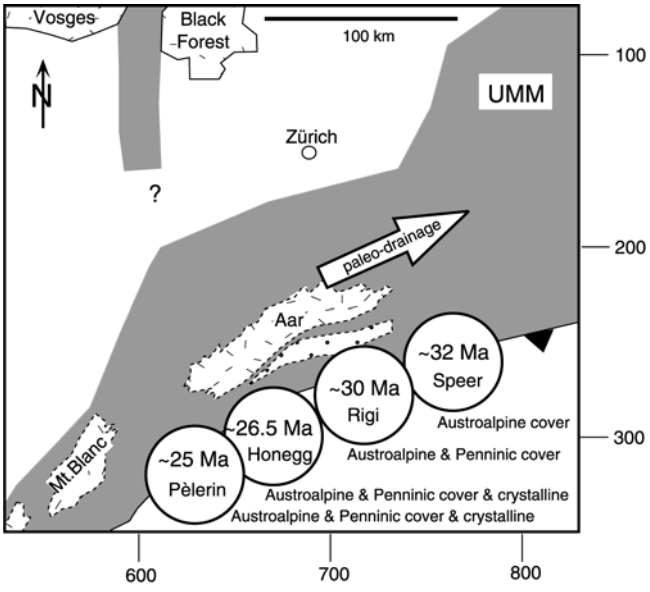

Figure 5. Distal pinch-out of the Lower Marine Molasse group (UMM), dispersion direction during UMM times, and spatial pattern of the first occurrence of thick-bedded conglomerates within the Molasse basin. Note the westward shift in time. The earliest pebbles are derived from the highest tectonic units (Austroalpine cover nappes). Younger pebbles witness incision into underlying units (crystalline of Austroalpine and Penninic nappes). Grid numbers refer to the Swiss national kilometer grid.

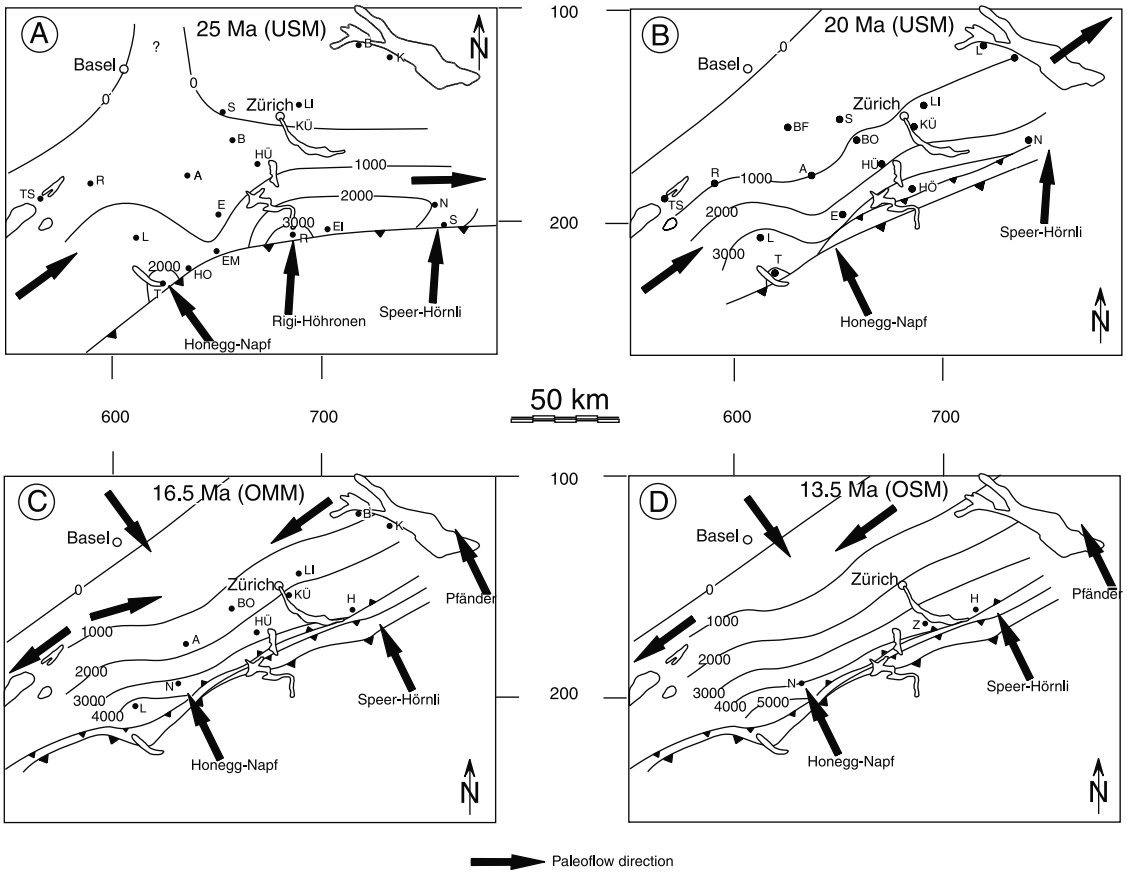

Figure 6. Depth to base of foreland strata (in 1000 m intervals), interpreted in terms of deflection of the North European foreland plate, and paleoflow direction. Note the westward migration of the location of enhanced deflection in time and the switch from east directed to west directed paleoflow orientations (black arrows). Abbreviations of wells are explained in Table 1.

indicates the directions of the axial drainage for these times. At 25 Ma, maximum deflections of 3000 m occurred in the east, whereas the contemporaneous magnitude of deflection measured significantly less in the west (~2000 m) (Figure 6a). The distal part of the basin included an area of reduced subsidence as indicated by the arcuate curvature of the 1000 m isopach. Despite this irregularity, paleoflow directions at 25 Ma were east directed, suggesting an eastward tilt of the topographic axis of the basin. We anticipate that this tilt was caused by the deflection of the foreland plate. The flexural pattern of the foreland plate then changed in the early Miocene as indicated by the nearly uniform magnitude of maximum deflection (3000–4000 m) in the east and in the west (Figure 6b and 6c). Parallel to this, paleoflow orientation changed from an eastward direction to a situation with no preferred dispersion direction (Figure 6c). This conclusion is based on the stratigraphic studies by *Berger* [1996] and *Keller* [1989], who revealed that at circa 20 Ma the transgression of the peripheral shallow sea prograded from the Paratethys in the east and the Tethys in the west. Both transgressional tips finally met in the area of Zürich sometime after 20 Ma.

[30] During deposition of the Upper Marine Molasse group (OMM), however, the subsidence pattern of the foreland plate changed, and deflection was enhanced in the west (as opposed to enhanced deflection in the east during the late Oligocene; Figure 6a). This westward shift of the location of increased subsidence rates is indicated by the asymmetry of the contour lines of depth-to-base of the Molasse strata: at 16.5 Ma and thereafter (Figures 6c and 6d) the Molasse deposits were significantly thicker in the west (~5000 m at 16.5 Ma) than in the east (~3000–4000 m). This westward tilt of the foreland plate is likely to have initiated a westward tilt of the topographic axis of the basin. Indeed, during deposition of the upper part of the OMM the paleoflow directions changed toward the west.

5. Synoptic View of the Alpine Orogen and the North Alpine Foreland Basin

[31] In order to get a synoptic view of the orogenic processes going on at depth and the erosional processes at the surface, as well as the sedimentation linked to the North Alpine foreland basin, three paleogeographic maps were constructed for the time slices of 32, 25 and 15 Ma, i.e., the time from the early Oligocene to middle Miocene, englobing the collision between the European and Adriatic margin. The maps shown in Figure 7 were reconstructed using information about (1) the motion between the Eurasian and African plates that was determined by paleomagnetic data from the Atlantic ocean [*Dewey et al.*, 1989] and (2) the amount of convergence between the European and Adriatic margins during

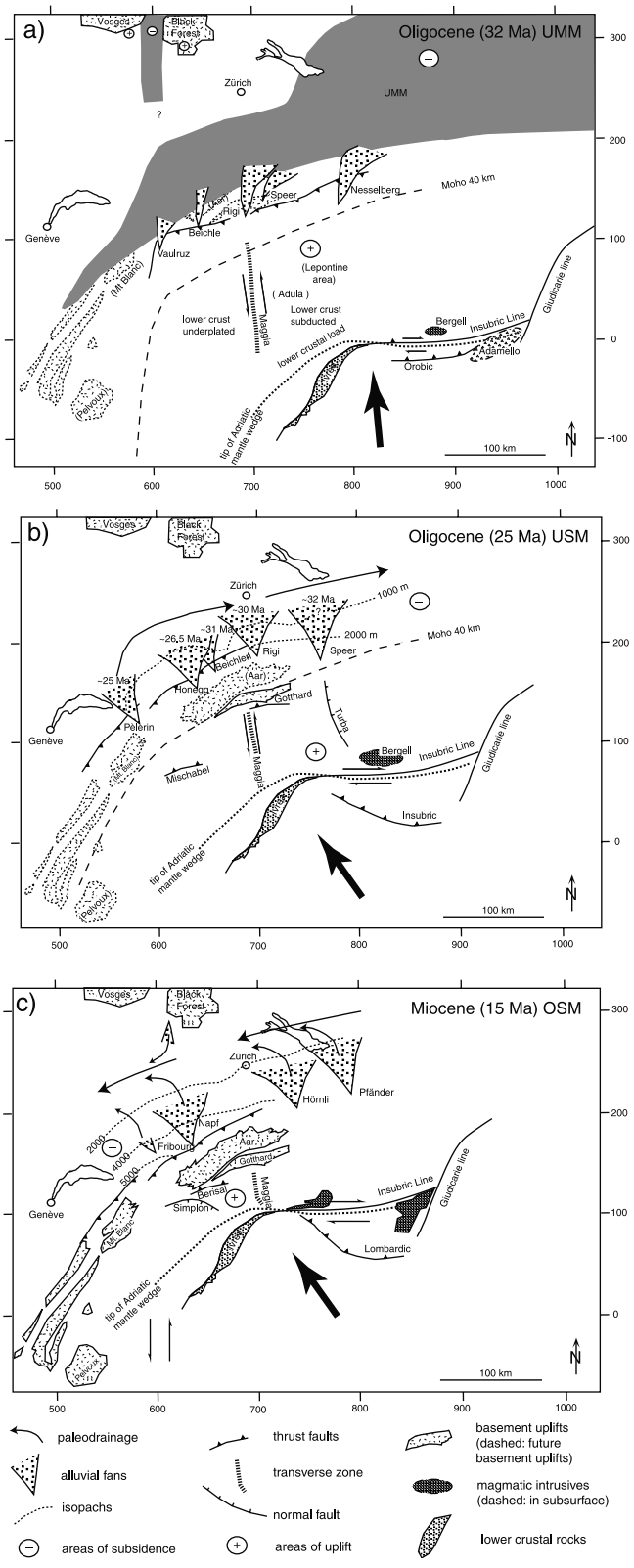

these time intervals that was determined from palinspastic reconstructions [*Pfiffner*, 1993b] and balancing of the Eastern Traverse [*Schmid et al.*, 1996, 1997]. The basement uplifts of the Black Forest and Vosges are reference points on the stable foreland. The outline of the external basement uplifts (Aar, Mont Blanc, Aiguilles Rouges, Belledonne, etc.) are taken as they appear on the geological maps and are not retrodeformed. The same applies for the outline of the Ivrea zone (a lower crustal section).

5.1. Early Oligocene

[32] Figure 7a shows the situation in Early Oligocene times at 32 Ma. The UMM sea to the north of the Alpine orogen extended from the Vienna Basin westward, narrowing down along the Swiss Alps to nearly zero width south of Geneva. The narrowing is also accompanied by a decrease in thickness of the sandy-shaly basin fill [*Pfiffner et al.*, 1997b], suggesting a lateral variation of flexing of the European plate at this time. A narrow sea extended southward within the Rhine graben whose opening is indicative of E–W extension in the Alpine foreland [*Ziegler*, 1987]. The occurrence of the first fan deltas shed into the UMM sea may suggest that the growing Alpine orogenic wedge had built up relief by this time.

[33] Within the Alpine orogen the Penninic nappe stack had already been formed and was undergoing thermal equilibration (Lepontine metamorphism). The tip of the European continent (Adula nappe) had been subducted to depths of around 80 km, had emerged from depth and was injected into the nappe pile [*Schmid et al.*, 1997]. Thickening of the crust in front of the Adriatic mantle wedge by underplating was likely to have produced surface uplift. The lower crustal substratum of the Penninic nappes was subducted beneath the Adriatic mantle wedge in the transect of the Lepontine area. Further west, however, it was partly stacked and underplated in front of the Adriatic mantle wedge.

[34] The structure of the Penninic nappes (upper crust) is different on either side of the Maggia transverse zone. This transverse zone includes the Maggia nappe and is characterized by orogen-normal strike and trend of foliations and stretching lineations [cf. *Merle et al.*, 1989]. The Maggia nappe itself has steeply dipping fault contacts striking orogen-normal, i.e., parallel to the likely transport direction of the Penninic nappes. We interpret this situation as a zone of wrench faulting between an eastern (Lepontine) and western nappe stack, which formed kinematically independent from each other.

Figure 7. (opposite) Paleogeographic sketch maps showing relative positions of key crystalline basement units (Black Forest on stable Europe, future basement uplifts Aar, Mont Blanc, etc., in external Alps, and Ivrea lower crustal section of Adriatic margin). (a) In Early Oligocene (32 Ma), convergence between the Adriatic and European margins caused important thrusting and exhumation (Lepontine) in the eastern Swiss Alps. Flexing of the European plate was responsible for the subsiding UMM sea to taper out toward the west. (b) In Late Oligocene (25 Ma) the Ivrea body and associated lower crustal wedge had moved westward by strike slip along the Insubric Line. Continued convergence led to the buildup of relief in the paleo-Alps. Shedding of conglomerates migrated westward. (c) By Late Miocene (15 Ma) the Ivrea body and lower crustal section had continued to move farther west. Subsidence in the Molasse Basin also migrated west and the paleodrainage now occurred to the west. Exhumation in the Alpine orogen due to surface erosion and normal faulting along the Simplon normal fault was mainly concentrated in the western Swiss Alps.

[35] At 32 Ma the Insubric Line acted as a steeply north dipping backthrust which exhumed the Penninic nappes, but in addition dextral strike slip motion was initiated. To the south of the Insubric Line, the Adamello intrusion had crosscut a preexisting thrust fault within the Southern Alps (the Orobic thrust; see *Schönborn* [1992]).

[36] The European crust-mantle boundary was dipping south beneath the Swiss Alps, but was dipping east beneath the Western (French-Italian) Alps. The curved shape of the Moho and the crustal root is indicated by the trace and location of the 40 km structure contour line.

[37] The tip of the Adriatic mantle wedge as determined from geophysical data trends E–W along the Insubric Line and more N–S in the Western Alps [*Nicolas et al.*, 1990; *Rey et al.*, 1990]. The latter orientation represents the orientation of the Jurassic spreading axis of the Piemont ocean, which had opened to the west of the Ivrea zone. The E–W strike of the Insubric Line appears to have been inherited from Cretaceous strike slip or maybe even from a Jurassic transform fault.

5.2. Late Oligocene

[38] Figure 7b shows the situation in Late Oligocene times at 25 Ma. By this time, the gravel fans had augmented in volume and prograded out into the Molasse Basin. Subsidence progressed from east to west, as indicated by the westward shift of the location of enhanced rates of alluvial fan construction (shedding of conglomerates in Speer fan initiated at 32 Ma, at circa 30 Ma at Rigi, and from 25 Ma onward in the west). Isopachs suggest higher sediment thicknesses, i.e., more down-flexing, in the eastern part of the Molasse Basin (e.g., the 2000 m isopach is restricted to the Speer and Rigi fans).

[39] Within the orogen, N–S convergence led to the formation of the Helvetic nappes. The Insubric Line still acted as a steep backthrust accommodating strike slip motion. Coeval thrusting along the steeply north dipping Insubric Line and the gently south dipping thrust faults of the Helvetic nappes uplifted the plug in between (including the Lepontine area) causing surface uplift and relief. Rock uplift in the Lepontine area just north of the Adriatic mantle wedge was mainly restricted to the area east of the Maggia transverse zone, and this crustal thickening was counterbalanced by E–W extension along the east dipping Forcola normal fault.

[40] Within the growing wedge, crustal thickening was locally also achieved by backfolding (south of Gotthard and Mischabel in Figure 7b). South of the Insubric line, thrusting of the so-called Insubric phase propagated outward, extending the retrowedge [*Beaumont et al.*, 1999]. The area just SE of the Ivrea zone (and Ivrea body) lacks significant thrusting, possibly owing to the shield effect of the shallow strong mantle piece. Dextral strike slip related to oblique convergence moved the Adriatic mantle and associated lower crustal wedge toward the Western Alps, thereby loading and flexing the European plate. The shape change and northwestward shift of the 40 km structure contour line of the European Moho reflects this continued crustal thickening and lithosphere flexure.

5.3. Miocene

[41] Figure 7c shows the situation in Miocene times at 15 Ma. The OSM gravel fans had shifted farther out into the Molasse Basin. In addition, drainage was now toward the west, and the isopachs indicate higher subsidence rates in the west compared with the rates in the east. This tilt of the basin axis reflects additional loading of the western part of the Molasse Basin and the adjoining Alps. The Adriatic mantle and associated lower crustal wedge and the location of enhanced rates of crustal thickening (Figure 4) had moved farther west. Convergence migrated outward to include the external basement uplifts (Aar, Mont Blanc–Aiguilles Rouge, Belledonne massifs) and, ultimately, the Jura Mountains.

[42] Rapid rock uplift now affected the Penninic nappes located west of the Maggia transverse zone above the Toce culmination [*Merle et al.*, 1989]. This uplift and associated crustal thickening led to E–W extension along the west dipping Simplon normal fault.

[43] South of the Insubric line, the retrowedge widened by thrusting, which had propagated farther to the south (Lombardic phase). Oblique convergence is held responsible for continued dextral strike slip along the Insubric Line and sinistral strike slip in the Western Alps [*Ricou and Siddans*, 1986].

[44] Convergence continued after 15 Ma, in the course of which the entire Molasse Basin north of the Swiss Alps underwent a clockwise rotation by 7°–14° [*Kempf et al.*, 1998]. This rotation can be perceived as passive rotation of a piggyback basin, associated with folding and thrusting of the Jura Mountains. Shortening within the Jura Mountains increases in a sense compatible with the clockwise rotation. Out-stepping of the thrust front from the internal Molasse Basin to the external Jura Mountains incorporated the basin into the orogenic wedge. As a consequence, the basin fill was transported up along a gently dipping detachment fault and thus raised above base level, which led to yet another reorganization of the drainage system and even removal of parts of the basin fill [*Schlunegger et al.*, 1998].

6. Flexing the Foreland Plate: Role of the Adriatic Mantle Wedge

[45] The Adriatic wedge beneath the Central Alps comprises lower crustal and mantle lithosphere rocks. We examine the possibility that this wedge formed an extra crustal load in the Alps [*Rey et al.*, 1990] which may have caused enhanced deflection of the foreland plate [*Kahle et al.*, 1997].

[46] The Adriatic wedge was raised into a structurally high position in the course of Jurassic rifting and subsequent opening of the Piemont ocean. During Cretaceous E–W convergence, this ocean was closed and subducted eastward beneath this mantle wedge. The European plate west of the Western Alps was flexed into this east dipping subduction zone [*Rey et al.*, 1990]. Subsequent N–S convergence flexed the European plate north of the Swiss Alps down into a south dipping subduction zone. This created a curved depression in the plate, which made a bend of roughly 90° around the arc of the Western and Swiss Alps.

[47] We assess the relative influence of the subcrustal load that may arise from the Adriatic mantle and associated lower crustal wedge for a profile through eastern Switzerland (see Figure 1 for location). Restored sections of the foreland basin and the Alpine orogen at Oligocene (32 Ma) and Early Miocene times (19 Ma) are taken from *Pfiffner et al.* [2000]. The sections at these times constrain the northern pinch out of the foreland basin deposits, the position of the northern front of the paleo-Alps, as well as the shape of the European plate beneath the orogen as derived from

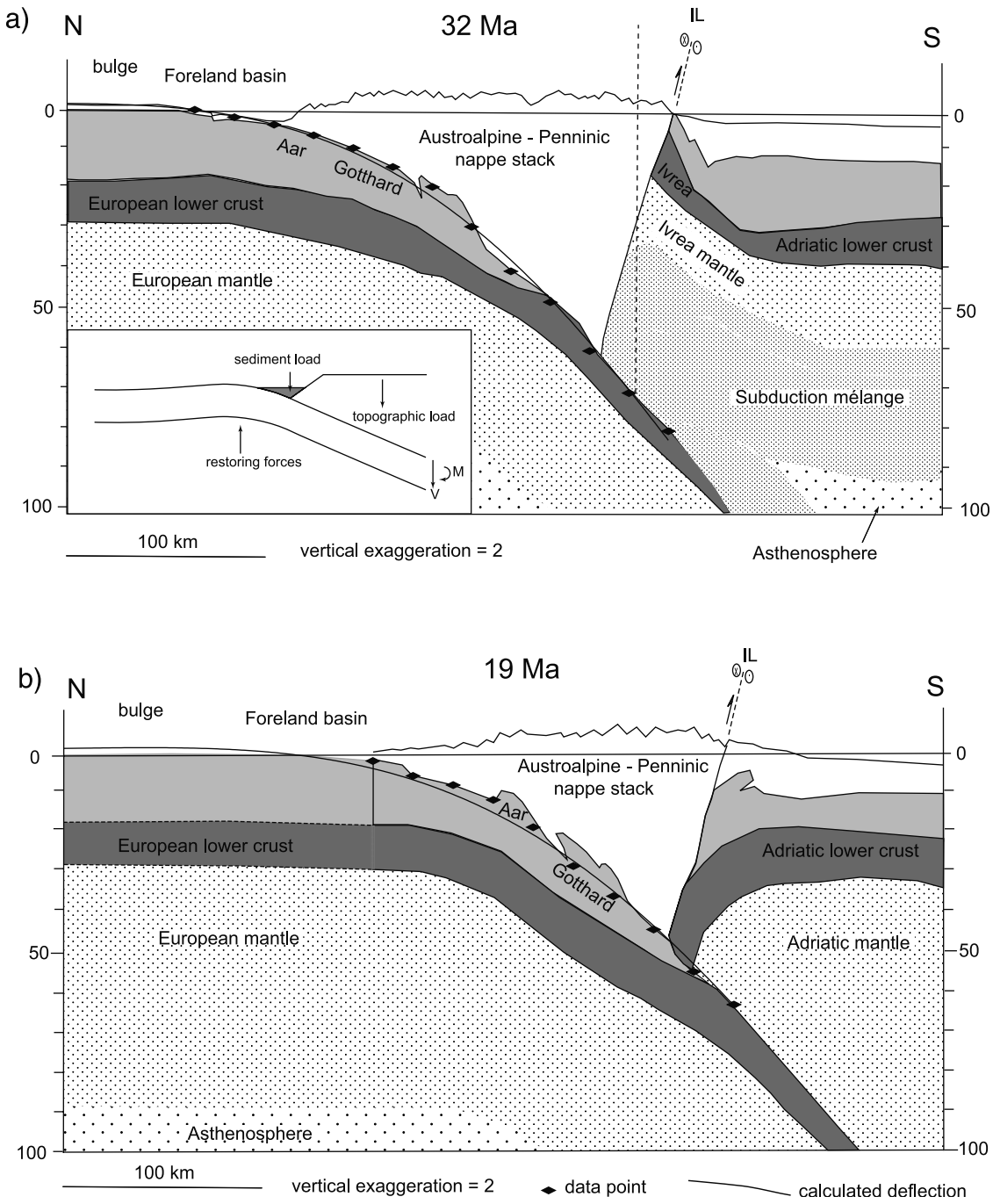

Figure 8. Analysis of flexure of the European plate for a section through eastern Switzerland. (a) Reconstructed geometry at 32 Ma [from *Pfiffner et al.*, 2000]. Note the Ivrea mantle wedge south of the Insubric Line (IL). The diamonds indicate data points which were used in the flexural modeling. The solid line is the calculated best fit to these data points. Modeling parameters include the following: Young's modulus 10^{11} Pa, Poisson's ration 0.25, gravitational acceleration of 9.81 m s^{-2}, sediment density of 2300 kg m^{-3}, mantle density of 3250 kg m^{-3}, density of topographic load of 2800 kg m^{-3} to the north of the dashed vertical line, and 3000 kg m^{-3} to the south of it. The best fit was obtained for an effective elastic thickness of 35 km, $M = 14 \times 10^{16}$ N and $V = 15 \times 10^{12}$ N m^{-1}. The inset shows the forces taken into account in the flexural modeling. (b) Reconstructed geometry at 19 Ma [from *Pfiffner et al.*, 2000]. Solid line now shows the calculated plate deflection if the extra load associated with the Adriatic mantle wedge is removed. Values of modeling parameters as in Figure 8a, except for the density of the topographic load, which is 2800 k gm^{-3} everywhere. The fit to the European plate deflection (indicated with diamonds) is remarkably good.

metamorphic and structural data from within the orogen. They also suggest that the European plate was flexed more at 32 Ma as compared to 19 Ma.

[48] Our approach is the following: We first search for a model that best fits the reconstructed deflection at 32 Ma. We then use this model to analyze the effect which the disappearance of the Adriatic mantle wedge may have had on the deflection.

6.1. Numerical Modeling of the European Plate Deflection

[49] To simulate the geometry of the down-flexed European foreland plate, we load an elastic, broken plate floating on a fluid substratum. We do not calculate a time evolution, but assume a static model which is representative for the situation at one time in the past. The modeling method which we use is described in more detail by *Buiter et al.* [1998]. The thickness of the flexed plate is an effective elastic thickness. This effective thickness is used to simulate the behavior of real lithosphere with a depth-dependent (continental) rheology. Previous analyses of the Swiss Alpine foreland deflection show a rather wide range, of 5–50 km, for the effective elastic thickness for this region [e.g., *Karner and Watts*, 1983; *Sinclair et al.*, 1991; *Royden*, 1993; *Stewart and Watts*, 1997; *Burkhard and Sommaruga*, 1998]. In our modeling, the effective elastic thickness is used as a free parameter.

[50] The foreland plate is deflected under various loads: (1) the load of topography (the Alpine thrust belt), (2) the load of sediments deposited in the foreland, (3) an extra (subsurface) load related to the Adriatic mantle and lower crustal wedge, and (4) an end load associated with the deeper part of the subducted slab, which is simulated through a bending moment (M) and a shear force (V).

[51] The topographic load included all material present between the topographic profile at the Earth's surface and the top of the subducting plate. Since the topography in the past is not known exactly, we use a constant elevation of 2 km which is comparable to the average value of the present-day situation. The sensitivity to this assumption is discussed in section 6.2. Sediments are present between the thrust belt and the forebulge to a depth of 5 km. They constitute a relatively small load. Water was not considered because we are dealing with a very shallow basin.

[52] We systematically vary the effective thickness of the elastic plate and the end load (both M and V) until a good fit to the reconstructed deflection geometry of the European foreland plate is obtained. This is somewhat similar to the approach taken by *Andeweg and Cloetingh* [1998] for the German-Austrian Molasse Basin, and differs from studies where the present-day geometry of Alpine foreland deflection is modeled [e.g., *Karner and Watts*, 1983; *Royden*, 1993; *Gutscher*, 1995; *Burkhard and Sommaruga*, 1998]. We use data points of the reconstructed foreland plate deflection down to depths of 60–80 km, which is well below the foreland basin depths considered in most plate flexure studies of this area. The fit is measured by a root-mean-square difference between calculated deflection and data.

[53] The first step in analyzing the effect of changes in loading of the foreland plate consists in finding a best fit to the reconstructed deflection at 32 Ma (Figure 8a). At that time, the Adriatic wedge (Ivrea body) was present in the region under consideration. We use a density of 2800 kg m^{-3} for the topographic load and simulate the denser Adriatic wedge through a higher density of 3000 kg m^{-3} which is applied uniformly with depth south of the location marked in the profile of Figure 8a. The best fit is obtained for an effective elastic thickness of 35 km (Figure 8a). The values of modeling parameters used are given in the caption to Figure 8. We obtained a good fit to the deflection data without having recourse to varying the value of effective elastic thickness laterally along the profile. The effect of lateral heterogeneities is discussed in section 6.2. We found that a good fit can be obtained for lower values of effective elastic thickness in case only shallower deflection data are used [e.g., *Sinclair et al.*, 1991; *Schlunegger et al.*, 1997; *Burkhard and Sommaruga*, 1998].

[54] The next step consists in evaluating the effect which the disappearance of the denser mantle wedge might have had on the plate deflection. Between 32 Ma and 19 Ma the wedge moved out of the section under consideration by dextral strike slip along the Insubric Line. We calculated the deflection at 19 Ma, using the same effective elastic thickness and the same deep load (M and V) as for 32 Ma. Given the absence of the Adriatic wedge, the density of the topographic load was taken as 2800 kg m^{-3} everywhere. The reduction in the topographic load clearly reduces the deflection of the foreland plate, as shown in Figure 8b.

[55] The final step consists in comparing the calculated shape of the model plate to the reconstructed deflection at 19 Ma. The fit between the two deflection profiles is remarkably good. It should be emphasized here that we have not sought to fit the 19 Ma deflection data. Rather, we just have examined the effect of a reduction in the topographic load, using the values for elastic thickness, bending moment and shear force as derived from the 32 Ma deflection geometry.

6.2. Sensitivity to Model Parameters

[56] There are parameters which are ill-defined by the geologic record and which might significantly affect our model results: topographic profile and possible lateral variations in elastic thickness and uncertainties. Another uncertainty concerns the dip of the flexed plate beneath the orogen. We calculated a series of models (not shown here) to explore the sensitivity of our results to these parameters and discuss them briefly.

[57] Our reference model uses an average elevation of 2 km for the orogen. This value is comparable to the present-day situation, which is characterized by an average elevation of 1700 m along the transect studied here [*Kühni and Pfiffner*, 2001]. There are no indications that the topography was significantly different in Oligocene or Miocene times. We therefore analyzed the cases with mean elevations of 1 km and 3 km, which we consider to represent lower and upper end-members. For both cases we found the influence of the change in elevation to be small. The parameters which yield a fit between the model and the restored geometry at 32 Ma (Figure 8a) also predict the shape of the restored geometry at 19 Ma (Figure 8b) with the mantle wedge removed. For mean elevations of 1 km the elastic thickness is calculated to be 35 km; for 3 km this value is 30 km.

[58] In another model series we addressed the uncertainty in the dip angle of the restored geometries at 32 Ma and 19 Ma. This uncertainty includes the error in pressure-temperature (p-T) conditions obtained from petrologic studies and the error inherent in not properly placing the samples (ore thrust sheets) of known p-T conditions upon retrodeformation. We estimate that the upper and lower bound for the error would place the southernmost data point

of the subducting slab 10 km higher, 10 km lower than the reference model at 32 Ma, respectively (Figure 8a). Again, we found that using the parameters obtained to fit the geometry at 32 Ma, the deflection at 19 Ma is mimicked rather accurately when the mantle wedge is removed. The elastic thickness for a steeper dip at 32 Ma is determined at a value of 35 km; at a shallower dip, it is determined at a value of 30 km.

[59] It could be argued that the elastic thickness might show lateral variations owing to tectonic thinning or weakening as a result of higher temperatures. We therefore replaced the homogeneous flexed slab of the reference model by a lateral variation in elastic thickness. It is to be expected that the effective elastic thickness decreases with depth, but we have no constraints for the magnitude of this decrease. Therefore we chose and present just one model out of the large number of imaginable variations. The elastic thickness at the southern end beneath the orogen is set to 50% of the value in the model foreland. We adopted a linear increase from 50% at the southern end to 100% over a distance of 120 km (i.e., the slab south of the bulge in Figure 8a). The best fit is obtained for an elastic thickness of 50 km (25 km at the southern end). The parameters determined to fit the model geometry at 32 Ma predict the shape at 19 Ma, with the mantle wedge removed, rather well.

[60] In all our calculations the Adriatic wedge only loads the end of our plate, and it could be argued, therefore, that its effect cannot have been large. However, we are certain that there has been a reduction in the total loading of the plate between 32 and 19 Ma. We deduce this from a separate calculation in which we sought a best fit for the 19 Ma deflection, i.e., by varying the end load (M and V). The loads obtained for this best fit are smaller than the loads for the 32 Ma best fit, indicating that the total load was reduced.

[61] We thus conclude that the conclusions drawn from the reference model are robust and that the presence of the Adriatic mantle wedge significantly influenced the steepness of the flexed subducting European plate in Oligocene and Miocene times.

7. Conclusions

[62] Oblique convergence with associated dextral strike slip along the Insubric Line displaced the Adriatic wedge westward relative to the European plate. Our compilation reveals that within the same time interval the location of maximum subsidence in the Molasse Basin, as indicated by the thicknesses of the accumulated sediments, also migrated westward, and that the drainage pattern changed from an easterly flow to a westerly flow of paleorivers. This coincidence in time and space is explained by flexing of the European plate associated with the extra deep lithospheric load represented by the Adriatic wedge.

[63] Oblique convergence is also held responsible for the shift of the locus of rock uplift, surface uplift and denudation in the metamorphic part of the orogen. Exhumation of the Lepontine area occurred in response to collision at a time when the Adriatic wedge was located immediately to the south of the uplifting area in Oligocene times. Later, Miocene exhumation in the Toce area was caused by the same Adriatic wedge which had moved farther west in the meantime. In both metamorphic cores, rock and surface uplift involved crustal shortening by nappe stacking and back thrusting along the Insubric Line. The difference in nappe structure within these two areas points toward an independent kinematic evolution. As a consequence, the Maggia transverse zone, which marks the border between these two areas, evolved and compensated the necessary shear strains.

[64] Convergence between the Adriatic margin and the subducting European plate led to crustal thickening and, associated with shortening, positive relief (surface uplift), which in turn created topographic loads. These loads are held responsible for a further down-flexing and shaping of the foreland basin. We interpret the generation of relief by an adjustment to critical taper geometry [*Dahlen*, 1984]. Down-flexing increased the basal slope, which required an increase in the surface slope, which in turn increased river gradients and erosion. Thus the triggering of shedding of pebbles in the foreland basin, and its migration along the orogen, is intimately linked to the effects of crustal shortening.

[65] It appears therefore that the Swiss Alps are an orogen showing how crustal processes exert a first-order control on surface processes. Lithospheric loads (mantle and lower crustal wedges) influenced the shape of the European plate deflection, but also the buildup of relief by crustal shortening and nappe stacking, and ultimately the nature of the sedimentary infill and timing of basin formation.

[66] **Acknowledgments.** This paper was supported by the Swiss National Science Foundation (20–43, 246.95) and the Deutsche Forschungsgemeinschaft (SCHL 518/1–1). Special thanks go to A. Anspach (University of Jena) for technical assistance, and for construction of Figure 5. The constructive discussions with J. Melzer and H. von Eynatten (University of Jena) are kindly acknowledged. This paper benefited from comments by Wilfried Winkler and two anonymous reviewers.

References

Andeweg, B., and S. Cloetingh, Flexure and "unflexure" of the North Alpine German-Austrian Molasse Basin: Constraints from forward tectonic modeling, in *Cenozoic Foreland Basins of Western Europe*, edited by A. Mascle et al., *Geol. Soc. Spec. Publ., 134*, 403–422, 1998.

Beaumont, C., S. Ellis, and O. A. Pfiffner, Dynamics of subduction-accretion at convergent margins: Short-term modes, long-term deformation, and tectonic implications, *J. Geophys. Res.*, *104*, 17,573–17,601, 1999.

Berger, J. P., Cartes paléogéographiques-palinspastiques du bassin molassique suisse (Oligocène inférieur-Miocène moyen), *Neues Jahrb. Geol. Palaeontol. Abh.*, *202*, 1–44, 1996.

Bertotti, G., V. Picotti, and S. Cloetingh, Lithospheric weakening during "retroforeland" basin formation: Tectonic evolution of the central South Alpine foredeep, *Tectonics*, *17*(1), 131–142, 1998.

Buiter, S. J. H., M. J. R. Wortel, and R. Govers, The role of subduction in the evolution of the Apennines foreland basin, *Tectonophysics*, *296*, 249–268, 1998.

Burkhard, M., and A. Sommaruga, Evolution of the western Swiss Molasse basin: Structural relations with the Alps and the Jura belt, in *Cenozoic Foreland Basins of Western Europe,* edited by A. Mascle et al., *Geol. Soc. Spec. Publ., 134*, 279–298, 1998.

Channell, J. E. T., Paleomagnetic data from Umbria (Italy): Implications for the rotation of Adria and Mesozoic apparent polar wander paths, *Tectonophysics*, *216*, 365–378, 1992.

Dahlen, F. A., Noncohesive critical Coulomb wedges: An exact solution, *J. Geophys. Res.*, *89*, 10,125–10,133, 1984.

Dewey, J. F., M. L. Helman, E. Turco, D. H. W. Hutton, and S. D. Knott, Kinematics of the western Mediterranean, in *Alpine Tectonics*, edited by M. P. Coward, D. Dietrich, and R. G. Park, *Geol. Soc. Spec. Publ., 45*, 265–284, 1989.

Diem, B., Die untere Meeresmolasse zwischen der Saane (Westschweiz) und der Ammer (Oberbayern), *Eclogae Geol. Helv.*, *79*, 493–559, 1986.

Escher, J. C., M. Hunziker, H. Marthaler, H. Masson, M. Sartori, and A. Steck, Geologic framework and structural evolution of the Western Swiss-Italian Alps, in *Deep Structure of the Swiss Alps: Results of NRP 20*, edited by O. A. Pfiffner et al., pp.

205–222, Birkhäuser Boston, Cambridge, Mass., 1997.

Froitzheim, N., P. Conti, and M. van Daalen, Late Cretaceous, synorogenic, low-angle normal faulting along the Schlinig fault (Switzerland, Italy, Austria) and its significance for the tectonics of the Eastern Alps, *Tectonophysics*, *280*, 267–293, 1997.

Füchtbauer, H., Sedimentpetrographische Untersuchungen in der älteren Molasse nördlich der Alpen, *Eclogae Geol. Helv.*, *57*, 157–298, 1964.

Gutscher, M., Crustal structure and dynamics in the Rhine Graben and Alpine foreland, *Geophys. J. Int.*, *122*, 617–636, 1995.

Homewood, P., P. A. Allen, and G. D. Williams, Dynamics of the Molasse Basin of western Switzerland, in *Foreland Basins*, edited by P. A. Allen and P. Homewood, *Spec. Publ. Int. Assoc. Sedimentol., 8*, 199–217, 1986.

Kahle, H.-G., et al., Recent crustal movements, geoid and density distribution: Contribution from integrated satellite and terrestrial measurements, in *Deep Structure of the Swiss Alps: Results of NRP 20*, edited by O. A. Pfiffner et al., pp. 251–259, Birkhäuser Boston, Cambridge, Mass., 1997.

Karner, G. D., and A. B. Watts, Gravity anomalies and flexure of the lithosphere at mountain ranges, *J. Geophys. Res.*, *88*, 10,449–10,477, 1983.

Keller, B., Fazies und Stratigraphie der Oberen Meeresmolasse (Unteres Miozän) zwischen Napf und Bodensee, Ph.D. thesis, Univ. of Bern, Bern, Switzerland, 1989.

Kempf, O., and A. Matter, Magnetostratigraphy of the eastern Swiss OSM, *Eclogae Geol. Helv.*, *92*, 97–104, 1999.

Kempf, O., F. Schlunegger, P. Strunck, and A. Matter, Paleomagnetic evidence for late Miocene rotation of the Swiss Alps: Results from the north Alpine foreland basin, *Terra Nova*, *10/1*, 6–10, 1998.

Kempf, O., A. Matter, D. W. Burbank, and M. Mange, Depositional and structural evolution of a foreland basin margin in a magnetostratigraphic framework: The eastern Swiss Molasse Basin, *Int. J. Earth Sci.*, *88*, 253–275, 1999.

Klaper, E. M., A discussion of contour maps in the Toce subdome of the Penninic realm (Switzerland, Italy), *Schweiz. Mineral. Petrogr. Mitt.*, *70*, 349–360, 1990.

Kühni, A., and O. A. Pfiffner, The relief of the Swiss Alps and adjacent areas and its relation to lithology and structure: Topographic analysis from a 250-m DEM, *Geomorphology*, *41*, 285–307, 2001.

Lihou, J. C., and P. A. Allen, Importance of inherited rift margin structures in the early North Alpine Foreland Basin, Switzerland, *Basin Res.*, *8*, 425–442, 1996.

Lyon-Caen, H., and P. Molnar, Constraints on the deep structure and dynamic processes beneath the Alps and adjacent regions from an analysis of gravity anomalies, *Geophys. J. Int.*, *29*, 19–32, 1989.

Mancktelow, N. S., Neogene lateral extension during convergence in the central Alps: Evidence from interrelated faulting and backfolding around the Simplonpass (Switzerland), *Tectonophysics*, *215*, 295–317, 1992.

Matter, A., P. Homewood, C. Caron, D. Rigassi, J. Van Stujivenberg, M. Weidmann, and W. Winkler, Flysch and molasse of western and central Switzerland, in *Geology of Switzerland, A Guidebook, Part B, Excursions*, edited by R. Trümpy, pp. 261–293, Schweiz. Geol. Komm., Wepf, Basel, 1980.

Merle, O., P. R. Cobbold, and S. Schmid, Tertiary kinematics in the Lepontine dome, in *Alpine Tectonics* edited by M. P. Coward, D. Dietrich, and R. G. Park, *Geol. Soc. Spec. Publ.*, *45*, 113–145, 1989.

Meyre, C., D. Marquer, S. M. Schmid, and L. Ciancaleoni, Syn-orogenic extension along the Forcola fault: Correlation of Alpine deformations in the Tambo and Adula nappes (Eastern Penninic Alps), *Eclogae Geol. Helv.*, *91*, 409–420, 1998.

Nicolas, A., R. Polino, A. Hirn, R. Nicolich, and ECORS-CROP working group *Mém. Soc. Géol. Fr.*, *156*, 15–27, 1990.

Nievergelt, P., M. Liniger, N. Froitzheim, and R. Ferreiro Mählmann, Early to mid-Tertiary crustal extension in the central Alps: The Turba Mylonite Zone (Eastern Switzerland), *Tectonics*, *15*(2), 329–340, 1996.

Pfiffner, O. A., Evolution of the north Alpine foreland basin in the central Alps, in *Foreland Basins*, edited by P. A. Allen and P. Homewood, *Spec. Publ. Int. Assoc. Sedimentol.*, *8*, 219–228, 1986.

Pfiffner, O. A., Alpine orogeny, in *European Geotraverse*, edited by D. Blundell et al., pp. 180–189, Cambridge Univ. Press, New York, 1992.

Pfiffner, O. A., The structure of the Helvetic nappes and its relation to the mechanical stratigraphy, *J. Struct. Geol.*, *15*(3–4), 511–521, 1993a.

Pfiffner, O. A., Palinspastic reconstruction of the Pre-Triassic basement units in the Alps: The central Alps, in *Pre-Mesozoic Geology in the Alps*, edited by J. F. von Raumer and F. Neubauer, pp. 29–39, Springer-Verlag, New York, 1993b.

Pfiffner, O. A., and L. Hitz, Geologic interpretation of the seismic profiles of the Eastern Traverse (lines E1-E3, E7-E9): Eastern Swiss Alps, in *Deep Structure of the Swiss Alps: Results of NRP 20*, edited by O. A. Pfiffner et al., pp. 73–100, Birkhäuser Boston, Cambridge, Mass., 1997.

Pfiffner, O. A., E. M. Klaper, A.-M. Mayerat, and P. Heitzmann, Structure of the basement-cover contact in the Swiss Alps, *Mém. Soc. Géol. Fr.*, *156*, 247–262, 1990.

Pfiffner, O. A., P. Lehner, P. Heitzmann, S. Müller, and A. Steck (Eds.), *Deep Structure of the Swiss Alps: Results of NRP 20*, Birkhäuser Boston, Cambridge, Mass., 1997a.

Pfiffner, O. A., S. Sahli, and M. Stäuble, Structure and evolution of the external basement uplifts (Aar, Aiguilles Rouges/Mt. Blanc), in *Deep Structure of the Swiss Alps*: *Results of NRP 20*, edited by O. A. Pfiffner et al., pp. 139–153, Birkhäuser Boston,-Cambridge, Mass., 1997b.

Pfiffner, O. A., S. Ellis, and C. Beaumont, Collision tectonics in the Swiss Alps: Insight from geodynamic modeling, *Tectonics*, *19*(6), 1065–1094, 2000.

Rey, D., T. Quarta, P. Mouge, M. Miletto, R. Lanza, A. Galdeano, T. Carrozzuo, R. Bayer, and E. Armando, Gravity and aeromagnetic maps of the Western Alps: Contribution to the knowledge of the deep structures along the ECORS-CROP seismic profile, *Mém. Soc. Géol. Fr.*, *156*, 107–121, 1990.

Ricou, L. E., and A. W. B. Siddans, Collision tectonics in the Western Alps, in *Collision Tectonics* edited by M. P. Coward and A. C. Ries, *Geol. Soc. Spec. Publ., 19*, 229–244, 1986.

Royden, L. H., The tectonic expression of slab pull at continental convergent boundaries, *Tectonics*, *12*(2), 303–325, 1993.

Schlunegger, F., Controls of surface erosion on the evolution of the Alps: Contraints form the stratigraphies of the adjacent foreland basins, *Int. J. Earth Sci.*, *88*, 285–304, 1999.

Schlunegger, F., A. Matter, and M. A. Mange, Alluvial fan sedimentation and structure of the southern Molasse Basin margin, Lake Thun area, Switzerland, *Eclogae Geol. Helv.*, *86*, 717–750, 1993.

Schlunegger, F., D. W. Burbank, A. Matter, B. Engesser, and C. Mödden, Magnetostratigraphic calibration of the Oligocene to middle Miocene (30–15 Ma) mammal biozones and depositional sequences of the Swiss Molasse Basin, *Eclogae Geol. Helv.*, *89*, 753–788, 1996.

Schlunegger, F., T. E. Jordan, and E. M. Klaper, Controls of erosional denudation in the orogen on foreland basin evolution: The Oligocene central Swiss Molasse Basin as an example, *Tectonics*, *16*(5), 823–840, 1997.

Schlunegger, F., R. Slingerland, and A. Matter, Crustal thickening and crustal extension as controls on the evolution of the drainage network of the central Swiss Alps between 30 Ma and the present: Constraints from the stratigraphy of the North Alpine Foreland Basin and the structural evolution of the Alps, *Basin Res.*, *10*, 197–212, 1998.

Schmid, S. M., and E. Kissling, The arc of the Western Alps in the light of geophysical data on deep crustal structure, *Tectonics*, *19*(1), 62–85, 2000.

Schmid, S. M., O. A. Pfiffner, N. Froitzheim, and G. Schönborn, Geophysical-geological transect and tectonic evolution of the Swiss-Italian Alps, *Tectonics*, *15*(5), 1036–1064, 1996.

Schmid, S. M., O. A. Pfiffner, and G. Schreurs, Rifting and collision in the Penninic Zone of eastern Switzerland, in *Deep Structure of the Swiss Alps: Results of NRP 20*, edited by O. A. Pfiffner et al., pp. 160–185, Birkhäuser Boston, Cambridge, Mass., 1997.

Schönborn, G., Alpine tectonics and kinematic models of the central Southern Alps, *Mem. Sci. Geol.*, *1054*, 229–393, 1992.

Schumacher, M. E., G. Schönborn, D. Bernoulli, and H. P. Laubscher, Rifting and collision in the Southern Alps, in *Deep Structure of the Swiss Alps: Results of NRP 20*, edited by O. A. Pfiffner et al., pp. 186–204, Birkhäuser Boston, Cambridge, Mass., 1997.

Sinclair, H. D., Flysch to Molasse transition in peripheral foreland basins: The role of the passive margin versus slab breakoff, *Geology*, *25*, 1123–1126, 1997a.

Sinclair, H. D., Tectonostratigraphic model for underfilled peripheral foreland basins: An Alpine perspective, *Geol. Soc. Am. Bull.*, *109*(3), 324–346, 1997b.

Sinclair, H. D., and P. A. Allen, Vertical versus horizontal motions in the Alpine orogenic wedge: Stratigraphic response in the foreland basin, *Basin Res.*, *4*, 215–232, 1992.

Sinclair, H. D., B. J. Coakley, P. A. Allen, and A. B. Watts, Simulation of foreland basin stratigraphy using a diffusion model of Mountain belt uplift and erosion: An example from the central Alps, Switzerland, *Tectonics*, *10*(3), 599–620, 1991.

Stewart, J., and A. B. Watts, Gravity anomalies and spatial variations of flexural rigidity at mountain ranges, *J. Geophys. Res.*, *102*, 5327–5352, 1997.

Turcotte, D. L., and G. Schubert, *Geodynamics: Application of Continuum Physics to Geological Problems*, 650 pp., John Wiley, New York, 1982.

Valasek, P., The tectonic structure of the Swiss Alpine crust interpreted from a 2D network of deep crustal seismic profiles and an evaluation of 3D effects, Ph.D. thesis, Eidgenossische Technische Hochschule, Zurich, 1992.

Valasek, P., and S. Mueller, A 3D crustal model of the Swiss Alps based on an integrated interpretation of seismic refraction and NRP 20 seismic reflextion data, in *Deep Structure of the Swiss Alps: Results of NRP 20*, edited by O. A. Pfiffner et al., pp. 305–325, Birkhäuser Boston, Cambridge, Mass., 1997.

Waldhauser, F., E. Kissling, J. Ansorge, and J. Mueller, Three-dimensional interface modeling with two-dimensional seismic data: The Alpine crust-mantle boundary, *Geophys. J. Int.*, *135*, 264–278, 1998.

Ziegler, P. A., Late Cretaceous and Cenozoic intra-plate compressional deformation in the Alpine foreland, A geodynamic model, *Tectonophysics*, *137*, 389–420, 1987.

S. J. H. Buiter and O. A. Pfiffner, Institute of Geological Sciences, University of Bern, Baltzerstrasse 1, CH-3012 Bern, Switzerland. (Susanne@geo.unibe.ch; adrian.pfiffner@geo.unibe.ch)

F. Schlunegger, Geologisches Institut, Eidgenossische Technische Hochschule (ETH)-Zentrum, CH-8092 Zürich, Switzerland. (Fritz.Schlunegger@erdw.ethz.ch)